Three-dimensional electronic properties of multiple vertically stacked InAs / GaAs self-assembled quantum dots

Cite as: J. Appl. Phys. **100**, 063716 (2006); https://doi.org/10.1063/1.2353783
Submitted: 21 March 2006 • Accepted: 03 July 2006 • Published Online: 27 September 2006

J. H. Kim, J. T. Woo, T. W. Kim, et al.

Three-dimensional electronic properties of multiple vertically stacked InAs/GaAs self-assembled quantum dots

J. H. Kim, J. T. Woo, and T. W. Kim[a)]
Advanced Semiconductor Research Center, Division of Electronics and Computer Engineering, Hanyang University, 17 Haengdang-dong, Seongdong-gu, Seoul 133-791, Korea

K. H. Yoo
Department of Physics and Research Institute of Basic Sciences, Kyung Hee University, Seoul 137-701, Korea

Y. T. Lee
Department of Information and Communications, Gwangju Institute of Science and Technology, 1 Oryong-dong, Puk-gu, Gwangju 500-712, Korea

(Received 21 March 2006; accepted 3 July 2006; published online 27 September 2006)

The microstructural properties and the shape of an InAs/GaAs array grown by molecular beam epitaxy were studied using transmission electron microscopy (TEM) measurements, and the interband transitions were investigated by using temperature-dependent photoluminescence (PL) measurements. The shape of the InAs quantum dots (QDs) on the basis of the cross-sectional bright-field TEM image was modeled to be a convex-plane lens. The electronic subband energies and the wave functions were numerically calculated by using a three-dimensional finite-difference method, taking into account strain effects. The excitonic peaks corresponding to interband transitions from the ground electronic subband to the ground heavy-hole band (E_1-HH_1) in the multiple-stacked QDs, as determined from the PL spectra, were in reasonable agreement with the (E_1-HH_1) interband transition energies obtained from the results of the numerical calculations.
 [DOI: 10.1063/1.2353783]

I. INTRODUCTION

Self-assembled multiple-stacked InAs/GaAs quantum dots (QDs) have become interesting due to their potential applications in electronic and optoelectronic devices, such as single electron transistors,[1] infrared photodetectors,[2] and lasers.[3] Vertically stacked InAs/GaAs QD arrays have become particularly attractive because the enhanced QD density of the active region in the laser results in a decrease of the lasing threshold current.[4,5] Therefore, the size fluctuation substantially decreases due to the enhanced QD density,[6,7] and the optical properties of the QDs may become stabilized.[8] Even though studies concerning the electronic structure of the QDs are necessary for fabricating high-efficiency optoelectronic and electronic devices,[9] very few works have been done on the three-dimensional electronic structures of multiple-stacked InAs/GaAs QDs due to the inherent problems encountered with the complicated computation procedure.[10]

This paper reports the three-dimensional electronic properties of vertically stacked InAs/GaAs self-assembled QDs. The multiple-stacked InAs/GaAs QDs were grown by using molecular beam epitaxy (MBE). Transmission electron microscopy (TEM) and temperature-dependent photoluminescence (PL) measurements were performed to investigate the microstructural and the optical properties. The electronic subband energies and the corresponding energy wave functions in the InAs/GaAs QDs were calculated by using a three-dimensional finite-difference method (FDM) and an Arnoldi method.[11] The calculated interband transition energies were compared with the results of the PL spectra.

II. EXPERIMENTAL DETAILS

The samples used in this work were grown on semi-insulating (100)-oriented GaAs substrates by using MBE. Five periods of InAs self-assembled QD arrays were grown at 430 °C via the Stranski-Krastanow growth mode.[12] The multiple-stacked InAs/GaAs QD structure consisted of the following structures: a 250 Å GaAs capping layer, a 100 Å undoped $Al_{0.3}Ga_{0.7}As$ layer, a 300 Å Si-doped (3×10^{18} cm^{-3} modulation layer, an 80 Å undoped $Al_{0.3}Ga_{0.7}As$ spacer layer, a 150 Å undoped GaAs layer, five periods of undoped 1.6 monolayer InAs QDs/50 Å undoped GaAs capping layer acting as a barrier, a 1 μm undoped GaAs buffer layer, a superlattice layer of 20 periods of $Al_{0.3}Ga_{0.7}As$/GaAs, and a 1000 Å undoped GaAs buffer layer.

TEM observations were performed in a JEM 3010 transmission electron microscope operating at 300 kV. The samples for cross-sectional TEM measurements were prepared by cutting and polishing with diamond paper to a thickness of approximately 30 μm and then argon ion milling at liquid-nitrogen temperature to obtain electron transparency. PL measurements were carried out using a 75 cm monochromator equipped with a Ge detector. The excitation source was the 5145 Å line of an Ar^+-ion laser, and the sample temperature was controlled between 13 and 200 K by using a He displex system.

[a)]Author to whom correspondence should be addressed; electronic mail: twk@hanyang.ac.kr

III. THEORETICAL CONSIDERATION

The conduction band and the heavy-hole band structures are calculated by using the effective mass approximation, and the three-dimensional Schrödinger equation is given by

$$-\frac{\hbar^2}{2m^*}\left(\frac{\partial^2}{\partial x^2}+\frac{\partial^2}{\partial y^2}+\frac{\partial^2}{\partial z^2}\right)\varphi(x,y,z)+[V(x,y,z)-E]\varphi(x,y,z)=0, \quad (1)$$

where m^* is the effective mass of the electron or the heavy hole.[10] The model of the QD shape, on the basis of the TEM image, is a convex-plane lens, and the shape of the QDs can be expressed as

$$\cup_{i=0}^{4}\left\{(x,y,z):\frac{x^2}{(d_x/2)^2}+\frac{y^2}{(d_y/2)^2}+\frac{(z-i\cdot l)^2}{(d_z/2)^2}\leqslant 1,\ 0\leqslant z-i\cdot l\leqslant d_z\right\}, \quad (2)$$

where d_x, d_y, and d_z describe the axes of the ellipsoid, l is the vertical separation between the QDs, and i is an iteration integer number for the calculation of the five vertically stacked QDs. The potential energy for the electron in the QD is given by

$$V(x,y,z)=\begin{cases}E^*_{g,\mathrm{InAs}}r & (x,y,z)\in QDs\\ E^*_{g,\mathrm{GaAs}}r & (x,y,z)\notin QDs,\end{cases} \quad (3)$$

where $E_{g,\mathrm{InAs}}$ and $E_{g,\mathrm{GaAs}}$ are the energy gaps of InAs and GaAs, respectively, r is the conduction-band offset ratio (r_c), and $(1-r_c)$ is the valence-band offset ratio. For convenience of computation, the potential energy is defined as in Eq. (3).

Since the InAs QD is relatively flat, a simplified strain is employed by adding the following terms to the potential energy in Eq. (3): $a_c(\varepsilon_{xx}+\varepsilon_{yy}+\varepsilon_{zz})$ for the conduction band and $a_v(\varepsilon_{xx}+\varepsilon_{yy}+\varepsilon_{zz})+(b/2)(\varepsilon_{xx}+\varepsilon_{yy}-2\varepsilon_{zz})$ for the valence band, where $\varepsilon_{xx}=\varepsilon_{yy}=(a_{\mathrm{eq}}-a_L)/a_L$ and $\varepsilon_{zz}=-(2c_{12}/c_{11})\varepsilon_{xx}$. a and b are the deformation potentials, c_{11} and c_{12} are the elastic moduli, a_L is the lattice constant of each material, and a_{eq} is the equilibrium lattice constant of the QD structure, which is the same as the lattice constant of the GaAs bulk.[13]

The Schrödinger equation is numerically solved by using three-dimensional FDM. The meshes consist of cubes of the same size for convenience of computations. Therefore, the simplified differential equation becomes

$$\varphi(x+\delta,y,z)+\varphi(x,y+\delta,z)+\varphi(x,y,z+\delta)+\varphi(x-\delta,y,z)+\varphi(x,y-\delta,z)+\varphi(x,y,z-\delta)-6\varphi(x,y,z)+\frac{2m^*\delta^2}{\hbar^2}[V(x,y,z)-E]\varphi(x,y,z)=0. \quad (4)$$

We take the material parameters at each mesh containing the boundary surface to be the average values of the neighboring meshes. Then, the matrix becomes Hermitian with this implementation of the boundary conditions.

The wave function in the region far from the QDs should be zero. This boundary condition is implemented by assuming that the wave function becomes zero on the surface of a rectangular box of dimensions $L_x=L_y$ and L_z. In order to reduce the memory size, we used sparse matrix algorithms and data structures with a compressed column storage format, such the Harwell-Boeing format,[14] and to obtain accurate eigenvalues and eigenfunctions within a reasonable time, we employed an implicitly restarted Arnoldi method, which is a kind of invariant subspace iteration.[11]

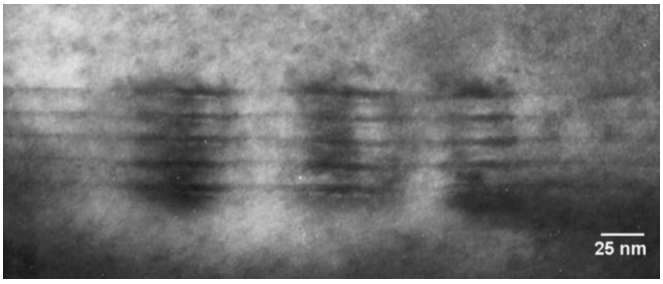

FIG. 1. Cross-sectional bright-field transmission electron microscopy image of five stacked InAs quantum dots embedded in GaAs barriers.

IV. RESULTS AND DISCUSSION

The result of the cross-sectional bright-field TEM for the five-period multiple-stacked InAs/GaAs QDs is shown in Fig. 1. Five periods of multilayers of InAs QDs arrays are embedded in each intrinsic GaAs barrier. These results are in reasonable agreement with those obtained by using atomic-force microscopy and plane-view bright-field TEM measurements. The QDs are relatively flat with typical diameters in the range of 20–25 nm and heights of about 12 nm. Since a QD might be isotropic in the plane perpendicular to the growth direction, it can be modeled by a half-ellipsoid.

Temperature-dependent PL spectra in the range of 13–200 K are shown in Fig. 2. Broad peaks are observed at all temperatures. While the dominant peak corresponds to the

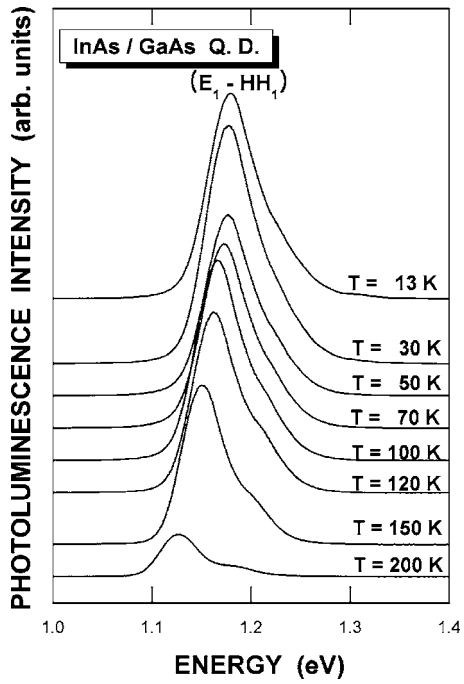

FIG. 2. Photoluminescence spectra measured at several temperatures for the InAs/GaAs QD arrays.

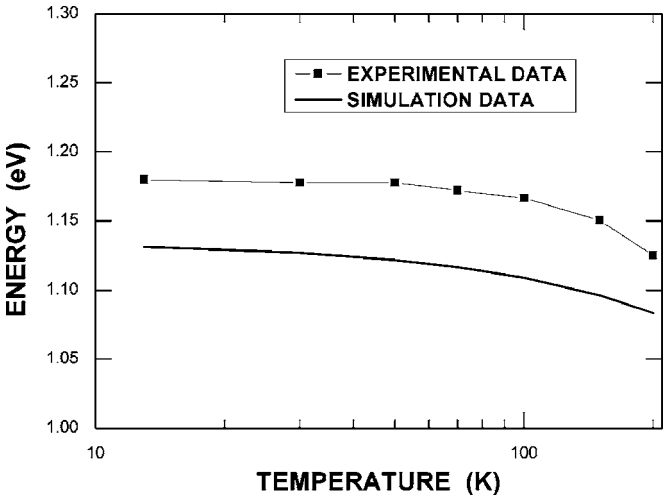

FIG. 3. Excitonic peaks corresponding to the (E_1-HH_1) transitions determined by using the temperature-dependent PL spectra (solid rectangles) and calculated by using the finite-difference method (solid line).

ground electronic subband to the ground heavy-hole band (E_1-HH_1) excitonic transition in the InAs/GaAs QDs, the shoulder at 200 K might be attributed to the first excited electronic subband to the first excited heavy-hole band (E_2-HH_2) transition in the QDs. The broadness of the peaks might originate from the transitions between higher energy states of the QDs. The (E_1-HH_1) peak position as a function of the temperature is plotted in Fig. 3. The peak position shifts to lower energy with increasing temperature because the energy gap of the InAs QDs increases with decreasing temperature, and the peak intensity decreases.

The band and the strain parameters of the InAs and the GaAs in the energy level calculation are summarized in Table I.[13,15]. The temperature-dependent energy gaps (E_g) of the InAs and the GaAs were obtained by linear interpolation of the values at 0 and 300 K. The r_c was taken to be 0.6. The QD shape parameters used in this calculation were d_x =245 Å, d_y=240 Å, d_z=24 Å, and l=50 Å. The axes d_x and the d_y of the QDs were assumed to be the same. However, a small difference between the d_x and the d_y was introduced to minimize numerically the instability due to the symmetry of the QD shape and to make the visualization of the wave

TABLE I. Physical parameters used for the calculation of the electronic structures of the multiple-stacked InAs/GaAs QDs.

Physical parameters		Materials	
		InAs	GaAs
Effective mass (m^*)	Electrons	0.023	0.067
	Heavy holes	0.4	0.5
Band gap E_g (eV)	0 K	0.417 14	1.514 883
	300 K	0.413 4	1.509 5
Deformation potential (a)		1.00	1.16
Deformation potential (b)		−1.8	−1.7
Elastic modulus (c_{11})		8.329	11.879
Elastic modulus (c_{12})		4.526	5.376
Lattice constant		6.058 4	5.653 3

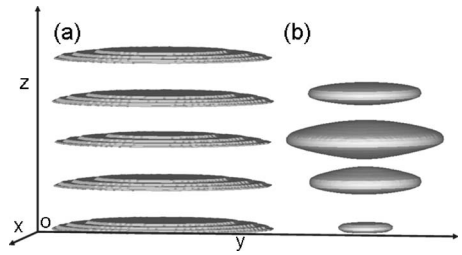

FIG. 4. (a) Finite-difference method meshes in the InAs QD region and (b) an isosurface of the ground conduction state wave function corresponding to $|\varphi|^2$=0.0027. O indicates the reference point and x, y, and z represent three-dimensional Cartesian coordinates.

function clearer. The dimensions of the rectangular box were taken to be L_x=L_y=306 Å and L_z=276 Å. The mesh size of the unit cell was $3\times3\times3$ Å^3, and a $957{,}168\times957{,}168$ sparse matrix was generated. The FDM meshes of the QDs, together with the rectangular box, are shown in Fig. 4(a).

The ground conduction-band energy was 0.853 eV and the heavy-hole energy was −0.278 eV. When one QD at the center is considered, the ground conduction-band energy is 0.893 eV, indicative of a coupling behavior between the QDs. The wave function for the ground conduction state is shown by a contour plot in Fig. 4(b). Such coupling effects of the wave functions for the QDs have already been observed in one-dimensional heterostructures.[16] Since the ground state probability for the top InAs QD is significantly smaller than those for the other InAs QDs due to the asymmetric shape of the stacked QDs with a half-ellipsoid, resulting in a decrease in the ground state probability for the top InAs QD in comparison with the corresponding probability for the lower QDs, that of the top InAs QD does not appear in Fig. 4(b).

The E_1-HH_1 transition energies at several temperatures were calculated and compared with the PL peak positions corresponding to E_1-HH_1 transitions in Fig. 3. The energy difference between the experimental and the theoretical results is about 0.05 eV, which can be attributed to the exciton binding energy. The temperature dependence trends of the calculated transition energy and the PL peak positions are similar. A more exact calculation can be achieved by taking into account three-dimensional strain effects and the interdiffusion behavior between the QD boundaries, which are not considered in this work.

V. SUMMARY AND CONCLUSIONS

Vertically stacked five-period InAs/GaAs QD arrays were grown by using MBE. The microstructural properties and the shape of the InAs/GaAs QD arrays were investigated by using cross-sectional bright-field TEM measurements, and the excitonic transitions were observed by using temperature-dependent PL measurements. The shape of the InAs QDs was that of a convex-plane lens, and the shape parameters were estimated from the TEM image. The electronic subband energy and the corresponding energy wave functions were numerically calculated by using a FDM. The calculated (E_1-HH_1) transition energy was in reasonable agreement with the (E-HH) transition energy obtained in the

PL measurement. These results can help improve understanding of the three-dimensional electronic properties of multiple-stacked InAs/GaAs QDs.

ACKNOWLEDGMENTS

This work was supported by the Korea Science and Engineering Foundation through the Quantum-functional Semiconductor Research Center at Dongguk University, and the work was also supported by a grant (Code No. 06K1501-02510) from the Center for Nanostructured Materials Technology under 21st Century Frontier R&D Programs of the Ministry of Science and Technology, Korea.

[1]E. Leobandung, L. Guo, Y. Wang, and S. Y. Chou, Appl. Phys. Lett. **67**, 938 (1995).
[2]S. Maimon, E. Finkman, G. Bahir, S. E. Schacham, J. M. Garcia, and P. M. Petroff, Appl. Phys. Lett. **73**, 2003 (1998).
[3]L. Harris, D. J. Mowbray, M. S. Skolnick, M. Hopkinson, and G. Hill, Appl. Phys. Lett. **73**, 969 (1998).
[4]B. Ilahi, L. Sfaxi, F. Hassen, B. Salem, G. Bremond, O. Marty, L. Bouzaiene, and H. Maaref, Mater. Sci. Eng., C **26**, 374 (2006).
[5]N. N. Ledentsov *et al.*, Phys. Rev. B **54**, 8743 (1996).
[6]A. S. Bhatti, M. Grassi Alessi, M. Capizzi, P. Frigeri, and S. Franchi, Phys. Rev. B **60**, 2592 (1999).
[7]H. Kissel, U. Müller, C. Walther, W. T. Masselink, Yu. I. Mazur, G. G. Tarasov, and M. P. Lisitsa, Phys. Rev. B **62**, 7213 (2000).
[8]G. G. Tarasov *et al.*, J. Appl. Phys. **88**, 7162 (2000).
[9]A. J. Williamson and A. Zunger, Phys. Rev. B **59**, 15819 (1999).
[10]P. Harrison, *Quantum Wells, Wires, and Dots: Theoretical and Computational Physics* (Wiley, New York, 2000).
[11]D. C. Sorensen, SIAM J. Matrix Anal. Appl. **13**, 357 (1992).
[12]D. Leonard, K. Pond, and P. M. Petroff, Phys. Rev. B **50**, 11687 (1994).
[13]S. L. Chuang, *Physics of Optoelectronic Devices* (Wiley, New York, 1995).
[14]E. Montagne and A. Ekambaram, Inf. Process. Lett. **90**, 87 (2004).
[15]*Semiconductors-Basic Data*, 2nd ed., edited by O. Madelung (Springer-Verlag, Berlin, 1996).
[16]J. T. Woo, J. H. Kim, T. W. Kim, J. D. Song, and Y. J. Park, Phys. Rev. B **72**, 205320 (2005).